Published as: *Science*. 2008 September 12; 321(5895): 1507–1510.

Conformational Switch of Syntaxin-1 Controls Synaptic Vesicle Fusion

Stefan H. Gerber[1,9,+], **Jong-Cheol Rah**[2,3,9,+], **Sang-Won Min**[1,9,+], **Xinran Liu**[1,4], **Heidi de Wit**[6], **Irina Dulubova**[5], **Alexander C. Meyer**[3], **Josep Rizo**[5,7], **Marife Arancillo**[2], **Robert E. Hammer**[5,7], **Matthijs Verhage**[6], **Christian Rosenmund**[2,3,*], and **Thomas C. Südhof**[1,4,8,9,*]

[1]Dept. of Neuroscience, UT Southwestern Medical Center, Dallas, TX 75390-9111 USA [2]Dept. of Molecular & Human Genetics and Neuroscience, Baylor College of Medicine, Houston TX 77030, USA [3]Dept. of Membrane Biophysics, Max-Planck-Institute for Biophysical Chemistry, 37077 Göttingen, Germany [4]Dept. of Molecular Genetics, UT Southwestern Medical Center, Dallas, TX 75390-9111 USA [5]Dept. of Biochemistry, UT Southwestern Medical Center, Dallas, TX 75390-9111 USA [6]Dept. of Functional Genomics, Vrije Universiteit, Amsterdam, The Netherlands [7]Dept. of Pharmacology, UT Southwestern Medical Center, Dallas, TX 75390-9111 USA [8]Dept. of Howard Hughes Medical Institute, UT Southwestern Medical Center, Dallas, TX 75390-9111 USA

Abstract

During synaptic vesicle fusion, the SNARE-protein syntaxin-1 exhibits two conformations that both bind to Munc18-1: a 'closed' conformation outside the SNARE-complex, and an 'open' conformation in the SNARE-complex. Whereas SNARE-complexes containing 'open' syntaxin-1 and Munc18-1 are essential for exocytosis, the significance of 'closed' syntaxin-1 is unknown. Here, we generated knockin/knockout mice that expressed only 'open' syntaxin-1B. Syntaxin-1B^{Open} mice were viable, but succumbed to generalized seizures at 2-3 months of age. Binding of Munc18-1 to syntaxin-1 was impaired in syntaxin-1B^{Open} synapses, and the size of the readily-releasable vesicle pool was decreased, whereas the rate of synaptic vesicle fusion was dramatically enhanced. Thus, the closed conformation of syntaxin-1 gates the initiation of the synaptic vesicle fusion reaction, which is then mediated by SNARE-complex/Munc18-1 assemblies.

Intracellular membrane fusion reactions are carried out by interactions between SNARE- and SM-proteins (for 'Soluble NSF-Attachment Protein Receptors' and 'Sec1-Munc18 like proteins'; *1,2*). In Ca^{2+}-triggered exocytosis in neurons and neuroendocrine cells, fusion is catalyzed by formation of SNARE complexes from syntaxin-1, SNAP-25, and synaptobrevin/vesicle-associated membrane protein, and the binding of the SM-protein Munc18-1 to these SNARE complexes (*1-3*). Syntaxin-1 consists of two similar isoforms (syntaxin-1A and -1B) that are composed of an N-terminal α-helical domain (the H_{abc}-domain) and a C-terminal SNARE-motif and transmembrane region. Outside of the SNARE-complex, syntaxin-1 assumes a 'closed' conformation in which the H_{abc}-domain folds back onto the C-terminal SNARE motif (*4,5*). In the SNARE-complex, by contrast, syntaxin-1 is 'opened' (*6*). Munc18-1 interacts with syntaxin-1 alone in the 'closed' conformation to form heterodimers (*3,4*), and additionally binds to SNARE-complexes

*Corresponding authors (tcs1@stanford.edu).
[9]Present addresses: Abt. Innere Medizin III, Universität Heidelberg, Germany (S.H.G.); Developmental Synaptic Plasticity Unit, NINDS, Bethesda, MD 20892 (J.-C. R.); UCSF Mission Bay Campus (S.-W.M.); Dept. of Molecular & Cellular Physiology and Neuroscience Institute, Stanford University (T.C.S.)
[+]These authors contributed equally

containing syntaxin-1 in the 'open' conformation to form SNARE-complex/Munc18-1 assemblies (*7,8*) which are essential for exocytosis (*3*). The significance of the closed conformation of syntaxin-1 and its binding to Munc18-1 remain unknown.

We used gene targeting to create mice that lack syntaxin-1A (syntaxin-1A^{KO}), and contain the 'LE' mutation in syntaxin-1B which renders it predominantly open (syntaxin-1B^{Open}; Fig. S1 [*9*]). Studying littermate offspring from crosses of double-heterozygous syntaxin-1A^{KO} and -1B^{Open} mice, we found that homozygous syntaxin-1A^{KO} mice exhibited no decrease in survival (Fig. 1A) or other obvious phenotypes (Figs. S2 and S3). The expendability of syntaxin-1A was unexpected in view of its high concentrations and proposed central functions (e.g., *10-14*), indicating that syntaxin-1A may be functionally redundant with syntaxin-1B.

Homozygous mutant syntaxin-1B^{Open} mice were also viable, but severely ataxic, and developed lethal epileptic seizures after 2 weeks of age (Figs. 1A and S3). The seizure phenotype of syntaxin-1B^{Open} mutant mice was recessive and independent of the syntaxin-1A^{KO}. Thus, syntaxin-1B was selectively essential, probably because it is more widely expressed than syntaxin-1A (*15*). In *C. elegans*, transgenic syntaxin-1^{Open} rescues the paralysis of unc-13 mutant worms (*16*), but crossing syntaxin-1B^{Open} mice with Munc13-1 knockout mice did not rescue the Munc13-1 knockout-induced lethality (Fig. S4).

The syntaxin-1A^{KO} mutation abolished syntaxin-1A expression (Fig. 1B), whereas the syntaxin-1B^{Open} mutation decreased syntaxin-1B levels (Fig. 1C). Both mutations produced a modest decrease in Munc18-1 levels, but no major changes in other proteins (Table S1). The syntaxin-1^{Open} mutation decreases formation of the Munc18-1–syntaxin-1 complex, but not formation of SNARE-complexes or Munc18-1–SNARE-complex assemblies (*3,8;* Fig. S5). Consistent with this conclusion, less Munc18-1 was co-immunoprecipitated with syntaxin-1 in syntaxin-1B^{Open} mice, whereas other SNARE-proteins co-immunoprecipitated normally (Figs. 1D and S6; note that SNARE-complex–Munc18-1 assemblies are not stable during immunoprecipitations, and thus cannot be evaluated).

Electron microscopy of cultured cortical neurons from littermate syntaxin-1B^{Open} and -1B^{WT} mice lacking syntaxin-1A revealed increased vesicle docking in syntaxin-1B^{Open} synapses (~25% increase; Figs. 2A-2D). The size of the postsynaptic density was also increased (~20%; Fig. 2E), while the density of docked vesicles per active zone length was unchanged (Fig. 2F). No other structural parameter measured differed between syntaxin-1B^{Open} and -1B^{WT} synapses; in particular, the number and intraterminal distribution of vesicles were unaltered (Fig. S7). In chromaffin cells, however, the syntaxin-1B^{Open} mutation caused a large decrease in chromaffin vesicle docking similar to the Munc18-1 knckout. Again, neither mutation altered the total number of chromaffin vesicles (Figs. 2K and 2L). Synaptobrevin-2 KO mice, analyzed in parallel as a negative control, did not change chromaffin vesicle docking, but increased the total number of chromaffin vesicles (Fig. 2L). Consistent with earlier findings (*17-20*), these results indicate that the Munc18-1–syntaxin-1 complex, but not the SNARE complex, functions in chromaffin vesicle docking. This function may not be apparent in vertebrate synapses because active zone proteins that are absent from chromaffin cells probably dock synaptic vesicles independent of their attachment to the Munc18-1–syntaxin-1 complex.

Measurements of spontaneous miniature excitatory postsynaptic currents (mEPSCs), of excitatory postsynaptic currents (EPSCs) evoked by isolated action potentials, and of use-dependent synaptic depression during high-frequency stimulus trains in hippocampal neurons revealed no significant difference between syntaxin-1A^{KO} and wild-type synapses (*12*). In syntaxin-1B^{Open} synapses (on the syntaxin-1A^{KO} background), however, the

mEPSC frequency was increased ~40%, and use-dependent depression of EPSCs was massively enhanced, although – surprisingly – evoked EPSCs exhibited a normal amplitude and kinetics (Fig. 3 and Fig. S8).

The increased depression in syntaxin-1B^{Open} synapses indicates that they exhibit a decreased readily-releasable vesicle pool (RRP), an increased release probability, and/or a decreased rate of refilling of the RRP after it is emptied. To test this, we measured the RRP by application of 0.5 M sucrose (*9,21*). The RRP was unchanged in syntaxin-1A^{KO} synapses, but decreased ~35% in syntaxin-1B^{Open} synapses (Figs. 4A and 4B), consistent with the decreased syntaxin-1 and Munc18-1 levels in syntaxin-1B^{Open} mice (Fig. 1C). Determination of the RRP size in the same synapses in which we monitored mEPSCs and evoked EPSCs (Figs. 3A-3F) allowed us to calculate the spontaneous vesicular release rate (as the ratio of mEPSC frequency to the RRP) and the vesicular release probability P_{vr} (as the ratio of EPSC and RRP charges). Both were increased >2-fold in syntaxin-1B^{Open} synapses (Figs. 4C and 4D), augmenting the percentage of the RRP released by a single action potential from ~10% in syntaxin-1B^{WT} to ~20% in syntaxin-1B^{Open} synapses. Measurements of the refilling rate of the RRP, however, detected an increase, and not a decrease (Fig. S9).

Thus, opening syntaxin-1 facilitates the fusion of synaptic vesicles on the background of a smaller RRP without changing the recruitment of vesicles into the RRP. Consistent with this conclusion, we found that the syntaxin-1B^{Open} mutation accelerates sucrose-induced release (Figs. 4E and 4F), and significantly boosts the relative amount and fractional release rate induced at lower sucrose concentrations (Figs. 4G-4I). Moreover, the syntaxin-1B^{Open} mutation increases the apparent Ca^{2+}-sensitivity of neurotransmitter release (Fig. S10), and occludes the phorbol-ester induced potentiation of release (Fig. S11). Overall, these results establish that although the RRP is smaller in syntaxin-1B^{Open} synapses, their resident RRP vesicles are more fusogenic.

Here, we show that the 'closed' conformation of syntaxin-1 performs three functions upstream of the canonical role of syntaxin-1 as a SNARE-protein in membrane fusion:

1. Closed syntaxin-1, but not the SNARE-complex, mediates vesicle docking in chromaffin cells, but not in synapses. The same differential phenotype is observed upon deletion of Munc18-1 (*17,18*), suggesting that the Munc18-1–syntaxin-1 complex docks chromaffin but not synaptic vesicles (see model in Fig. S12).
2. The closed syntaxin-1 conformation stabilizes syntaxin-1 and Munc18-1, whereas opening of syntaxin-1 decreases the syntaxin-1 and Munc18-1 levels, and thereby lowers the RRP size.
3. Most importantly, opening syntaxin-1 accelerates the rate of synaptic vesicle fusion, accounting for the fulminant epilepsy observed in synaxin-1B^{Open} mutant mice.

Ca^{2+} and sucrose trigger fusion of primed synaptic vesicles. Primed vesicles are thought to be suspended in a metastable state in which SNARE-complexes are assembled but the bilayers have not yet fused (*22*). We propose that primed vesicles are associated with a variable number of assembled SNARE-complexes, and that this number dictates the sucrose- and Ca^{2+}-sensitivity of a given vesicle (see model in Fig. S12). To account for the synaptic phenotype of syntaxin-1B^{Open} mutant mice, we hypothesize that the syntaxin-1B^{Open} mutation increases the average number of assembled SNARE-complexes per vesicle, and thereby enhances their Ca^{2+}- and sucrose-sensitivity. On the other hand, the destabilization of syntaxin-1 and Munc18-1 by the syntaxin-1B^{Open} mutation (Fig. 1) decreases the total number of primed vesicles and thus the RRP, even though the primed

vesicles are more fusogenic. The decrease in RRP is not due to the increased spontaneous release rate because its spontaneous fusion rate is still >100-fold lower than the vesicle repriming rate, and because much higher spontaneous fusion rates in synaptotagmin-mutant mice do not decrease the RRP size [*23*]). An alternative hypothesis would be that primed vesicles lack assembled SNARE-complexes, and Ca^{2+} or hypertonic sucrose trigger fusion of primed vesicles by inducing the opening of syntaxin-1 and assembly of SNARE-complexes (Fig. S12). The simplicity of this second model is attractive, but it cannot account for the speed of Ca^{2+}-triggered fusion, or for its dependence on complexin which binds to assembled SNARE complexes (*22*). Independent of which model is correct, our results demonstrate that syntaxin-1 performs multiple functions in exocytosis that go beyond its role as a SNARE-protein to include the control of vesicle docking and the regulation of the vesicle fusion rate.

Supplementary Material

Refer to Web version on PubMed Central for supplementary material.

Acknowledgments

We thank Ms. N. Hamlin, I. Kornblum, A. Roth, I. Herfort, and E. Borowicz for technical assistance. This work was supported by grants from the DFG (GE1042/1-1, GE1042/3-1, GE1042/3-2 to S.H.G.; Ro1296/5-3 to C.R.), the NIH (NS051262 to C.R., NS37200 to J.R.), and the NOSR (GpD970-10-036 and 900-01-001 to MV; 916-36-043 to HdW).

REFERENCES

1. Brunger AT. Q. Rev. Biophys. 2005; 9:1. [PubMed: 16336742]
2. Jahn R, Scheller RH. Nat Rev Mol Cell Biol. 2006; 7:631. [PubMed: 16912714]
3. Khvotchev M, et al. J. Neurosci. 2007; 27:12147. [PubMed: 17989281]
4. Dulubova I, et al. EMBO J. 1999; 18:4372. [PubMed: 10449403]
5. Misura KM, Scheller RH, Weis WI. Nature. 2000; 404:355. [PubMed: 10746715]
6. Sutton RB, Fasshauer D, Jahn R, Brunger AT. Nature. 1998; 395:347. [PubMed: 9759724]
7. Dulubova I, et al. Proc Natl Acad Sci U S A. 2007; 104:2697. [PubMed: 17301226]
8. Shen J, Tareste DC, Paumet F, Rothman JE, Melia TJ. Cell. 2007; 128:183. [PubMed: 17218264]
9. Experimental procedures are described in the Supplementary Online Materials
10. Bezprozvanny I, Scheller RH, Tsien RW. Nature. 1995; 378:623. [PubMed: 8524397]
11. Sheng ZH, Rettig J, Cook T, Catterall WA. Nature. 1996; 379:451. [PubMed: 8559250]
12. Naren AP, et al. Nature. 1997; 390:302. [PubMed: 9384384]
13. Deken SL, Beckman ML, Boos L, Quick MW. Nat. Neurosci. 2000; 3:998. [PubMed: 11017172]
14. Condliffe SB, Zhang H, Frizzell RA. J. Biol. Chem. 2004; 279:10085. [PubMed: 14703519]
15. Foletti DL, Lin R, Finley MA, Scheller RH. J. Neurosci. 2000; 20:4535. [PubMed: 10844023]
16. Richmond JE, Weimer RM, Jorgensen EM. Nature. 2001; 412:338. [PubMed: 11460165]
17. Verhage M, et al. Science. 2000; 287:864. [PubMed: 10657302]
18. Voets T, et al. Neuron. 2001; 31:581. [PubMed: 11545717]
19. Weimer RM, et al. Nat. Neurosci. 2003; 6:1023. [PubMed: 12973353]
20. de Wit H, Cornelisse LN, Toonen RF, Verhage M. PLoS. 2006; 1:e126.
21. Rosenmund C, Stevens CF. Neuron. 1996; 16:1197. [PubMed: 8663996]
22. Südhof TC. Annu. Rev. Neurosci. 2004; 27:509. [PubMed: 15217342]
23. Pang ZP, Sun J, Rizo J, Maximov A, Südhof TC. EMBO J. 2006; 25:2039. [PubMed: 16642042]

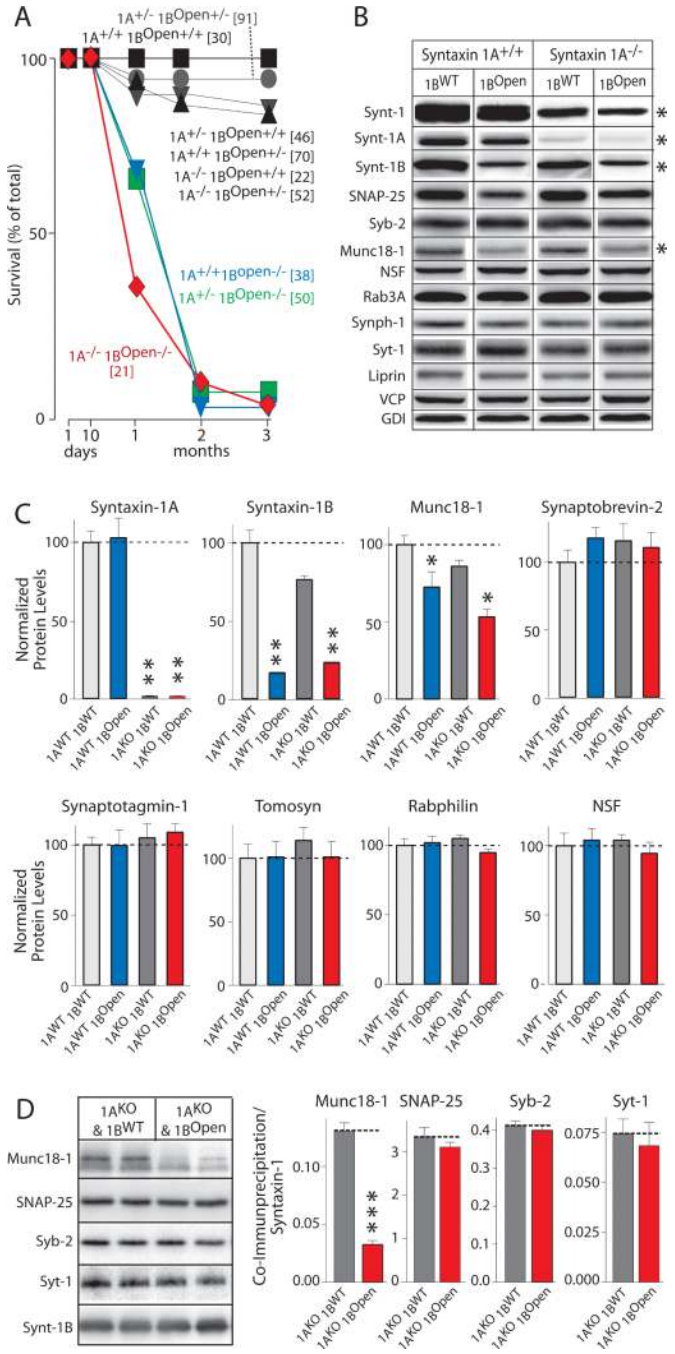

Figure 1. Syntaxin-1A^{KO}/syntaxin-1B^{Open} double mutant mice perish postnatally

A. Survival of syntaxin-1 mutant mice

B. and ***C***. Representative immunoblots (B) and levels of synaptic proteins (C) from syntaxin-1A^{WT}/1B^{WT}, -1A^{WT}/1B^{Open}, -1A^{KO}/1B^{WT}, and -1A^{KO}/1B^{Open} mutant mice determined by quantitative immunoblotting using ^{125}I-labeled secondary antibodies (see also Table S1).

D. Representative immunoblots (left) and quantitations (right) analyzing co-immunoprecipitation of Munc18-1, SNAP-25, synaptobrevin-2, and synaptotagmin-1 with syntaxin-1B^{WT} and -1B^{Open} in Triton X-100 solubilized brain proteins. The amounts of co-immunoprecipitated Munc18-1, SNAP-25, synaptobrevin-2, and synaptotagmin-1 were

determined by quantitative immunoblotting and normalized for the immunoprecipitated syntaxin-1.

Data in C and D are means ± SEMs; *=p<0.05; **=p<0.01; ***=p<0.001 by Student's t-test compared to wild-type. Abbreviations: Synt., syntaxin; Syb-2, synaptobrevin-2; Synph-1, synaptophysin-1; Syt-1, synaptotagmin-1; VCP, p97/vasolin-containing protein; GDI, GDP dissociation inhibitor.

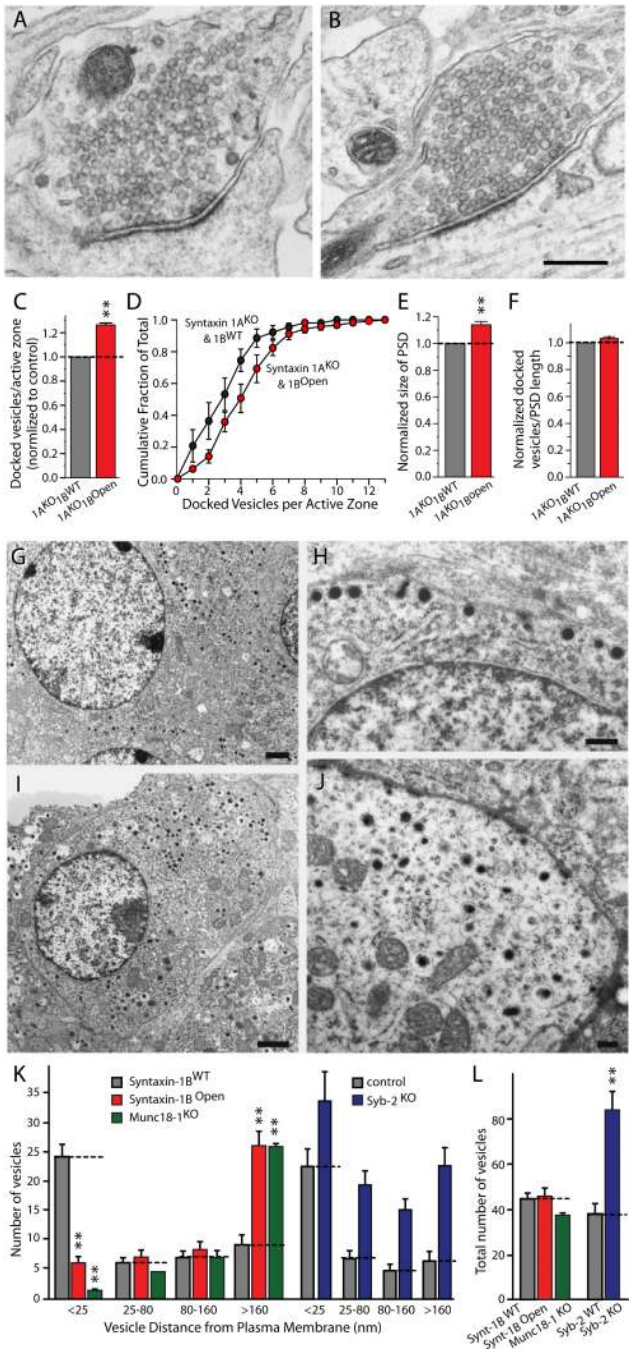

Figure 2. Syntaxin-1B^{Open} impairs chromaffin but not synaptic vesicle docking

A. and ***B***. Representative electron micrographs of neurons cultured from syntaxin-1A^{KO} mice containing wild-type syntaxin-1B^{WT} (A) or 'open' syntaxin-1B^{Open} (B; scale bar, 250 nm).

C. Number of docked vesicles per active zone (n = 3 experiments with 1B^{WT}=49, 55, and 32 synapses; 1B^{Open}=21, 38, and 49 synapses; normalized for wild-type values).

D. Plot of the cumulative distribution of docked vesicles per active zone (statistical significance with Kolmogorov-Simirnov test: $p<0.01$; 1B^{WT}=136, 1B^{Open}=108 synapses).

E. and ***F.*** Size of the postsynaptic density (E) and number of docked vesicles/length of postsynaptic density (F; both normalized for wild-type values).
G. - ***J.*** Representative electron micrographs of chromaffin cells from control (G,H) and syntaxin-1B^{Open} (I,J) littermate mice at embryonic day E18 at two magnifications (G,I: bar, 1 μm; H,J: bar, 200 nm).
K. Distribution of the distance of secretory granules from the plasma membrane in chromaffin cells from syntaxin-1B^{WT}, -1B^{Open}, Munc18-1 KO, and synaptobrevin-2 KO mice (analyzed separately with wildtype controls and binned as indicated).
L. Total number of secretory granules per chromaffin cell in syntaxin-1B^{WT} or -1B^{Open} mice, and in Munc18-1 and synaptobrevin-2 KO mice (K and L: N=3 animals, n = 60 chromaffin cells).
Data are means ± SEMs; **=p<0.01 by Student's t-test compared to wild-type.

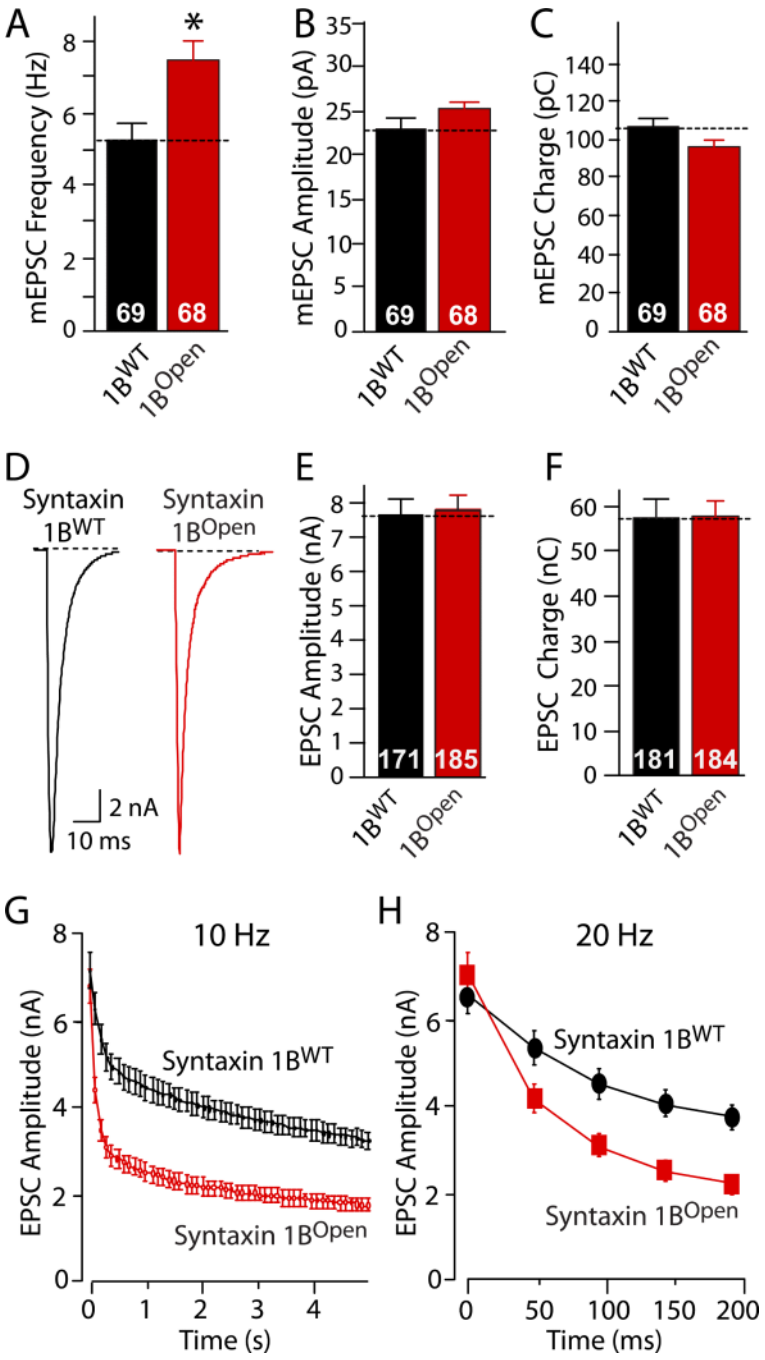

Figure 3. Neurotransmitter release in syntaxin-1B^{Open} synapses

A.- ***C***. Summary graphs of the frequency (A), amplitude (B), and charge (C) of spontaneous synaptic events (mEPSCs)

D. - F. Representative traces (D) and mean EPSC amplitudes (E) and charges (F) in synaptic responses induced by isolated action potentials

G. and ***H***. EPSC amplitudes of evoked synaptic responses elicited by 10 Hz (G) and 20 Hz stimulus trains (H).

Data are means ± SEMs; *=p<0.05 by Student's t-test compared to wild-type; numbers in bars show numbers of neurons analyzed.

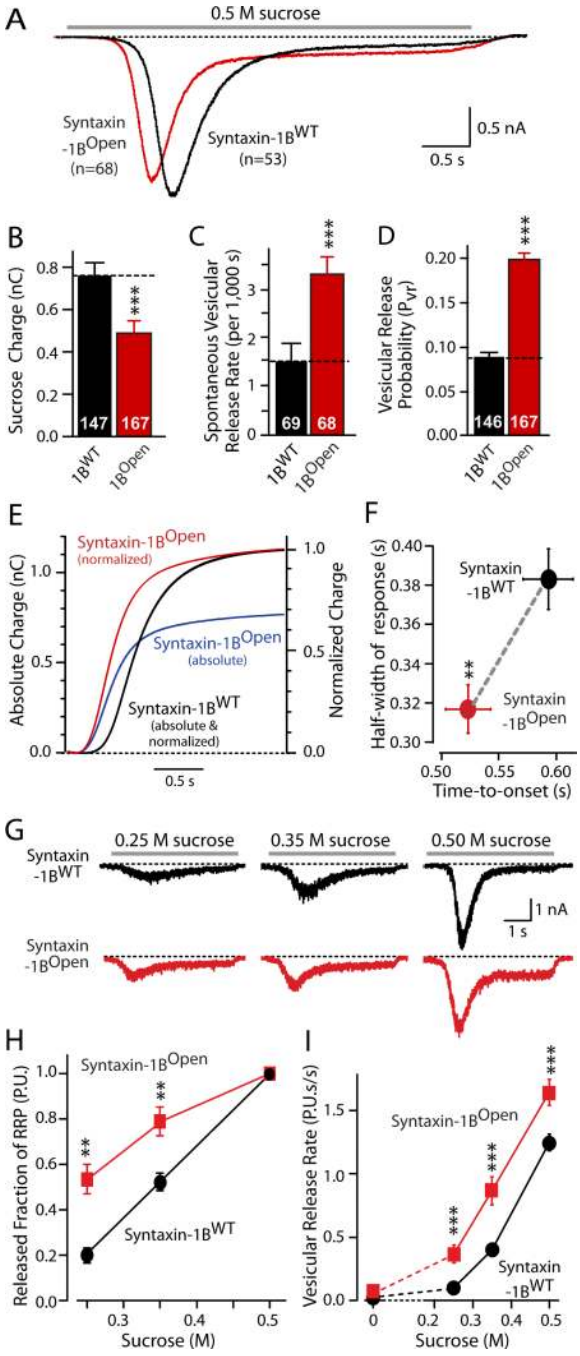

Figure 4. Increased fusogenicity of synaptic vesicles in syntaxin-1B^{Open} synapses

A. Average postsynaptic currents elicited by application of 0.5 M sucrose in syntaxin-1B^{WT} and -1B^{Open} synapses

B. Mean RRP size determined as the transient charge integral induced by application of 0.5 M hypertonic solution

C. Summary graph of the spontaneous vesicular release rate (mini frequency divided by the number of vesicles in the RRP)

D. Mean vesicular release probability (P_{vr} = evoked EPSC charge divided by the RRP charge).

E. Time-course of the average cumulative synaptic charge transfer during sucrose-induced release. For syntaxin-1B^{Open} synapses, both absolute (blue; left y-axis) and normalized responses (red; right y-axis) are depicted. In B and E, the steady-state component of release during the responses was subtracted.
F. Plot of the half-width vs. time-to-onset of sucrose-induced synaptic responses.
G. Representative traces of synaptic responses induced by 0.25 M, 0.35 M and 0.50 M sucrose.
H. and ***I***. Plot of the released fraction of the RRP (H; defined as the response to 0.5 M sucrose) and of the vesicular release rate (I) as a function of the sucrose concentration. In G, the 0 mM sucrose value represents the spontaneous vesicular release rate (Fig. 4D).
Data are means ± SEMs; **=p<0.01, ***=p<0.001 by Student's t-test compared to wild-type; numbers in bars show numbers of neurons analyzed.